#### **CHAPTER 188**

#### STOCHASTIC ANALYSIS OF OFFSHORE CURRENTS

Michel K. Ochi\* and Richard I. McMillen\*

#### ABSTRACT

This paper presents the results of stochastic analysis of offshore currents. The purpose of this study is to clarify the stochastic properties of offshore currents, and to develop a method to predict the magnitude of the extreme currents and their direction from measured data. Statistical analysis as well as spectral analysis are carried out on current velocities measured over a period of several months off Newfoundland, Canada. The effect of water depth on the statistical characteristics of current velocity is also clarified. The extreme current velocity expected to occur in 4- months and its direction are estimated by applying order statistics and the results are compared with the measured data.

#### INTRODUCTION

Current velocity measured in offshore areas, in general, results from currents primarily related with astronomical tide and those induced by local wind. Current velocity associated with ocean circulation and storm surge, etc., may also be significant depending on geographical location. All of these components can exist simultaneously, and hence the measured data demonstrate that the magnitude of the current velocity fluctuates in a random fashion with frequencies covering a wide range from 0.0008 to 0.08 cycles per hour (period range from 12 to 1200 hours).

Furthermore, the direction of the current velocity changes with time; it rotates clockwise in the northern hemisphere due to the rotation of the earth and the coriolis force. The angular frequency of rotation, however, is random. It varies from 0.31 to 0.70 radians per hour. Thus, the current velocity is considered to be a random process with varying frequency and direction.

Several studies have been carried out on the fluctuating properites of offshore currents as listed, among others, in References [1] through [8]. The results demonstrated in these references suggest that currents may be considered as a stochastic process consisting of various frequency components; (a) a tidal component with a frequency of 1 cycle per day (cpd) or 2 cpd depending on the location, (b) a wind-induced component with frequencies ranging from 0.10 to 0.20 cpd, and (c) seasonal variations of extremely low-frequency.

<sup>\*</sup> Coastal & Oceanographic Engineering Department University of Florida, Gainesville, Florida, U.S.A.

The purpose of the present study is to clarify the stochastic properties of offshore currents, and to develop a method to predict the magnitude of the extreme currents and their direction from measured data. For this, a statistical analysis is carried out on current velocities measured over a period of several months off Newfoundland, Canada. Statistical analysis as well as spectral analysis are carried out and the relationship between the area under the spectral density function and the variance evaluated from the time history is clarified. An analysis is also made of the data to examine the effect that water depth has on the statistical characteristics of current velocity. Finally, the extreme current velocity expected to occur in 4-months, and its direction, are estimated by applying order statistics and the results are compared with the measured data.

#### OFFSHORE CURRENT DATA AND ANALYSIS PROCEDURE

#### Data

Statistical analyses are carries out on approximately four months of continuous current data. The current meter mooring was located in a water depth of 84 meters. The mooring had three current meters sampling at 10 minute intervals at depths of 26, 47 and 75 meters. The current meter data are hourly mean velocities obtained by removing the high-frequency noise with a digital filter and sub-sampling the resulting smoothed signal to hourly values.

A dominant hourly current direction was obtained for each hourly current velocity from the directional data which was obtained from compasses moored with the current meters at the three depths. Here, the current direction is defined as that to which the water is flowing.

# Analysis Procedure

The time history of the near-surface current velocity is first decomposed into an East-West and North-South direction. An example of the time history of hourly current velocities as well as the decomposed East-West and North-South time histories are shown in Figure 1. This example represents the data obtained for two weeks from October 13 to October 27, 1981.

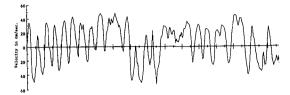
A statistical analysis is then performed on the East-West and North-South time histories in which the probability distributions applicable for deviations from the mean and the maximum (positive and negative variations) are obtained. After the statistical analysis is made for the East-West and North-South time histories, a Fast-Fourier-Transform (FFT) technique is used to obtain the energy spectrum for each time history.

In general, it is somewhat difficult to differentiate the measured current velocities into various components such as the wind- generated, tidal, and ocean current components, etc. Hence, it may be appropriate to decompose the measured currents into a high and low-frequency component. Here, the high-frequency component is considered to be the currents associated with tides, while the low-frequency components are those attributed to all other environmental conditions which may be called the residuals. The FFT is used to obtain the high-frequency (frequency > 0.035 cph) and the low-frequenct (frequency < 0.035 cph) current velocity time histories in the East-West and North-South directions. These are called the tidal and residual currents, respectively, in the present study.

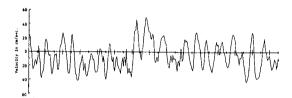
As an example, Figure 2 shows the time histories of the high-frequency (tidal) and the low-frequency (residual) current fluctuations for the East-West component which was shown in Figure 1.



Current velocity



East-west component of current velocity

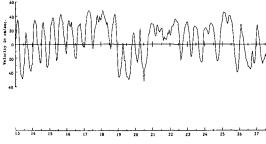


North-south component of current velocity

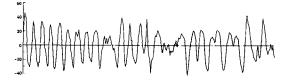
Figure 1: Time histories of current velocity, and East-West, and North-South components of velocity.

# RESULTS OF STATISTICAL ANALYSIS OF CURRENTS

Figure 3 shows an example of a polar diagram indicating the magnitude and direction of current velocity as a function of time. The data pertains to a 20-hour observation made on October 10th. The current velocities rotate clockwise in the Northern hemisphere through 360° in approximately 20 hours (a circular frequency of 0.31 radians per hour in this example. However, further analysis of the data indicates the circular frequency of the near- surface current is not constant, but instead varies from 0.31 to 0.70 radians per hour (9.0 to 20 hours). The circular frequencies of the current at 47 meter and 75 meter water depths are also examined. It is noted the preferred directions of motion water throughout the water column appears to be consistent with Ekman veering arguments.



East-west component of current velocity



High frequency (tidal) component of current velocity



Low frequency (residual) component of current velocity

Figure 2: Time histories of East-West component of current velocity, and high frequency (tidal) and low-frequency (residual) components.

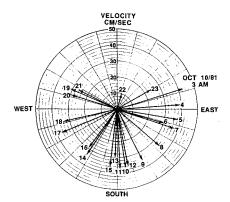


Figure 3: Current velocity magnitudes rotating in a clock-wise direction.

# Distribution of Fluctuating Current Velocities

Figure 4 shows the histograms of the deviations from the mean constructed from the time history for the East-West components. The deviations include both tidal and residual velocity components.

Included also in the figures are the normal (Gaussian) and non-Gaussian distributions for comparison with the histograms. The non-Gaussian probability density function is given by the following form of a Gram-Charlier expansion (Edgeworth [9] and Longuet-Higgins [10]):

$$f(x) = \frac{1}{\sigma\sqrt{2\pi}} \exp\left\{-\frac{x^2}{2\sigma^2}\right\} \left[1 + \frac{\lambda_3}{3!} H_3\left(\frac{x}{\sigma}\right) + \frac{\lambda_3^2}{72} H_6\left(\frac{x}{\sigma}\right) + \frac{\lambda_4}{4!} H_4\left(\frac{x}{\sigma}\right) + \ldots\right], \quad (1)$$

where  $\sigma^2$  = variance of current velocity,  $\lambda_3$  = skewness of the distribution,  $\lambda_4$  = kurtosis - 3,  $H_n\left(\frac{x}{\sigma}\right)$  = Hermite polynomial of degree n.

As can be seen in the figure, the distribution of the deviations from the mean value appears to follow a non-Gaussian probability distribution with parameter  $\lambda_4$  which is associated with the kurtosis of the distribution. The same trend can also be observed for deviations from the mean in the North-South current component.

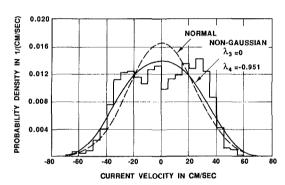


Figure 4: Histogram of deviations from the mean of East-West current velocity.

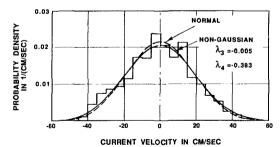


Figure 5: Histogram of deviations from the mean of tidal current velocity in East-West direction.

The correlation coefficient between two components (the East-West and North-South velocity components) is extremely small, on the order of 0.005. This implies that a statistical analysis of current velocities can be done independently in two directions.

Figures 5 and 6 show the histograms of deviations from the mean value for the tidal and residual components, respectively, in the East-West direction. Included also in these figures are the normal and non-Gaussian distributions for comparison with the histograms. As can be seen in these figures both the tidal and residual currents may be assumed to be Gaussian random processes. However, it will be shown later that the tidal component can be considered a narrow-band random process, while the residual component appears to be a non-narrow-band random process. This same trend can also be observed for currents in the North-South direction.

The results of computation show that the correlation coefficient between the tidal and residual currents is extremely small for both East-West and North-South directions. Therefore, it may safely be assumed that the tidal current and the residual current velocity components are statistically independent.

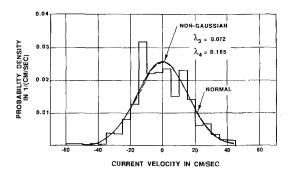


Figure 6: Histogram of deviations from the mean of residual current velocity in East-West direction.

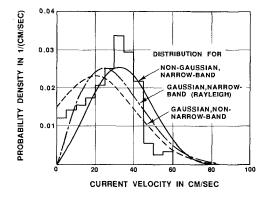


Figure 7: Histogram of maxima of current velocity in the East direction.

# Distribution of Maxima

Figure 7 shows the histogram of the maxima in the East direction constructed from current velocities including both tidal and residual components. Included also in the figure are the probability distributions applicable for the maxima. These include the probability density functions of the maxima applicable for a (a) narrow-band Gaussian random process, (b) non-narrow-band Gaussian random process, and (c) narrow-band non-Gaussian random process given below (Ochi & Wang [11]):

 $f(\xi) = \frac{1}{L} \left[ \frac{\xi}{\sigma^2} \exp\left\{ -\frac{\xi^2}{2\sigma^2} \right\} \left\{ 1 + \frac{\lambda_4}{4!} H_4(\frac{\xi}{\sigma}) \right\} \right]$  (2)

where  $\sigma^2$  = variance of current deviation from the mean  $\xi$  = maxima,  $0 < \sigma < \infty$ , L = normalization factor.

As can be seen in the figure, the histogram of the maxima, as expected, is not represented by either of the two distributions associated with a Gaussian (normal) process. The representation of the histogram by the probability distribution of the maxima for a non-Gaussian random process is marginally acceptable. A possible explanation of this discrepancy between the histograms and the distribution for the maxima of a non-Gaussian random process is as follows:

The distribution applicable for the maxima of a non-Gaussian random process (Equation 2) is developed based on the assumption that the process is narrow-banded. However, the time history of offshore currents including both tidal and residual components encompasses an extremely wide range of frequencies (from 0.0008 to 0.08 cycles per hour). This indicates that the maxima of the offshore currents (including both tidal and residual components) may obey the distribution applicable for a non-narrow-band, non-Gaussian random process.

# Spectral Analysis

Spectral analysis is carried out on measured current velocities to examine (a) frequency components which carry significant energy with the current flow, and (b) the relationship between spectral energy (area under the spectral density function) and the variance of the current fluctuations which can be evaluated from the time history of the current velocity. Figures 8 and 9 show the energy spectra for the tidal and residual components in the East-West direction, respectively. A Fast-Fourier-Transform technique is used to obtain the tidal and residual time histories in both the East-West and North-South directions. A cutoff frequency of 0.035 cycles/hour (28.4 hour period) is used to separate the time histories into their respective tidal and residual components.

The area under the spectral density function, denoted by  $m_o$ , and the bandwidth parameter, denoted by  $\varepsilon$ , are evaluated from the spectra and tabulated in Table 1. Included also in the table are the variances,  $\sigma^2$ , obtained from the time history of current velocity. It may be of interest to compare the variance,  $\sigma^2$ , with the moment,  $m_o$ . These should agree, in general for a weakly stationary, ergodic random process with zero mean. The offshore current velocity measured over a period of several months, however, cannot be considered as a stationary random process. Nevertheless, as can be seen in the table, the agreement between  $\sigma^2$  and  $m_o$  is reasonable in both the East-West and North-South directions. The

difference between them is approximately 8 percent in the East-West direction, and 4 percent in the North-South direction. The agreement between  $\sigma^2$  and  $m_o$  for the decomposed tidal and residual components is excellent. This is because the time histories of the tidal and residual components are obtained through FFT filtering techniques which retain the statistical properties of random phenomena including phase information as well.

The results obtained above substantiate the fact that the spectral density function of the current velocity in any direction is interrelated with the variance of current fluctuations. Hence, the probabilistic prediction of the magnitude of current velocity may be made through spectral analysis.

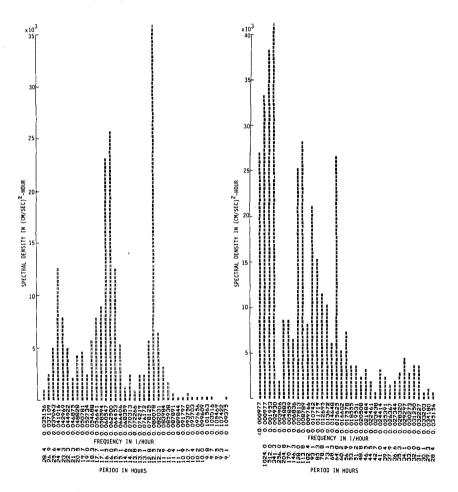


Figure 8: Energy spectrum of tidal (High frequency) current velocity in East-West direction.

Figure 9: Energy spectrum of residual (low frequency) current velocity in East-West direction.

Table 1: Variance evaluated from time history of current velocity,  $\sigma^2$ , area under the current energy spectrum, m, and spectrum band-width parameter,  $\epsilon$ .

Current velocity components East-West direction	Variance o <sup>2</sup>	Area under the spectrum <sup>m</sup> o	Spectrum band- width parameter ε
Total	627.5	583.2	0.735
Residual	248.6	248.7	0.845
Tidal	334.2	334.3	0.494
North-South direction			
Total	529.0	508.1	0.735
Residual	214.2	214.2	0.828
Tidal	293.6	293.7	0.505

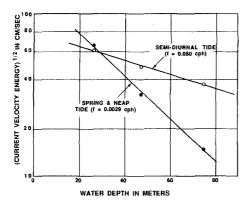


Figure 10: Square-root of current energy density for frequencies 0.080 cph (12.5 hour period) and 0.0029 cph (14.2 day period).

#### Effect of Water Depth

The same statistical analysis carried out on the near-surface current data was also made on data obtained at two deeper depths; 47 and 75 meters. These are called the mid-depth and near-bottom locations in the following analysis.

The results of the analysis indicate that almost all statistical properties of the fluctuating current velocity obtained from analysis of data at the deeper depths appear to be nearly the same as those obtained from the current velocities at the near surface. However, the severity of current fluctuations is drastically reduced with increase in depth, and the non-Gaussian random process characteristics observed for the near-surface current velocity are substantially less pronounced at deeper locations.

In order to examine the reduction of current velocity with increase in water depth, Figure 10 was prepared. The figure shows the square root of the current energy density (the vector sum of the East-West and North-South components) for the frequencies 0.080 cph (period 12.5 hours) and 0.0029 cph (period 341 hours) plotted on semi-log paper as a function of water depth. Here, the frequency 0.080 cph corresponds to that for the semi-diurnal tide, and the tidal current (high frequency) spectrum shows an extremely large energy density at this frequency. The frequency 0.0029 cph corresponds to that for the spring and neap tide, and the residual current (low frequency) spectrum shows considerable energy density at this frequency.

As can be seen in the figure, the square-root of current energy, which is proportional to the current velocity, reduces exponentially with increase in water depth. The reduction rate of the current velocity for the spring and neap tide (low-frequency) is much larger than that for the semi-diurnal tide (high-frequency component). This result indicates that the tidal and residual current energies both decrease substantially with increase in water depth. However, the rate of decrease for the residual currents is much larger than that for the tidal currents.

#### Estimation of Extreme Value

It was shown that the current velocity fluctuations can be considered as a non-Gaussian random process with the parameter  $\lambda_4$ , and that the East-West component and the North-South component are statistically independent. This being the case, it can be proved that the current velocity for an arbitrary direction is also approximately a non-Gaussian random process as derived in the Appendix. That is, the probability density function of current velocity fluctuations (deviation from the mean) for an arbitrary direction  $\theta$  can be given by Eq. (1) with  $\lambda_3=0$  and with the following variance,  $\sigma^2$ , and parameter,  $\lambda_4$ , which are now a function of angle  $\theta$ :

$$\sigma^{2}(\theta) = \sigma_{e}^{2} \sin^{2}\theta + \sigma_{n}^{2} \cos^{2}\theta$$

$$\lambda_{4}(\theta) = \frac{\lambda_{4e} \sigma_{e}^{4} \sin^{4}\theta + \lambda_{4n} \sigma_{n}^{4} \cos^{4}\theta}{\left(\sigma_{e}^{2} \sin^{2}\theta + \sigma_{n}^{2} \cos^{2}\theta\right)^{2}}$$
(3)

where  $\theta$  = angle measured from North to East,  $\sigma_e^2$ ,  $\sigma_e^2$  = variance of the East-West and North-South direction, respectively,  $\lambda_{4e}$ ,  $\lambda_{4n}$  = parameter  $\lambda_4$ -value for the East-West direction and North-South direction, respectively.

This results in the probability density function of the maxima having the same form as shown in Eq. (2) but with the variance,  $\sigma^2(\theta)$ , and parameter,  $\lambda_4(\theta)$ , as given in Eq. (3). That is,

$$f(\xi,\theta) = \frac{1}{L} \left[ \frac{\xi(\theta)}{\sigma^2(\theta)} \exp\left\{ -\frac{1}{2} \left( \frac{\xi(\theta)}{\sigma(\theta)} \right)^2 \right\} \left\{ 1 + \frac{\lambda_4(\theta)}{4!} H\left( \frac{\xi(\theta)}{\sigma(\theta)} \right) \right\} \right]$$
(4)

where  $L = 1 + \lambda_4(\theta)/3!$ 

Then, the extreme current velocity which is most likely to occur in n-peaks for a given angle  $\theta$ , denoted by  $\overline{\xi}(\theta)$ , is given as the value which satisfies the following equation:

$$\int_{0}^{\overline{\xi}(\theta)} f(\xi, \theta) d\theta = F(\overline{\xi}(\theta)) = 1 - \frac{1}{n}$$
 (5)

Numerical computations were carried out for various angles between 0 and 90 degrees, with variance  $\sigma_e^2 = 583.2 (\text{cm/sec})^2$  and  $\sigma_n^2 = 508.1 (\text{cm/sec})^2$ , and n = 175 in a 4-month observation period.

Figure 11 shows the computed extreme current velocities for various directions plotted in polar coordinates. As can be seen in the figure, there is no substantial difference in the magnitude of the extreme current velocities in various directions for data used in the present analysis. The magnitudes of the extreme current velocities in the shaded domain in the figure are nearly equal (70.3 - 69.6 cm/sec). The magnitude of the extreme current velocity observed in the same time period is 74.0 cm/sec in the South-West direction.

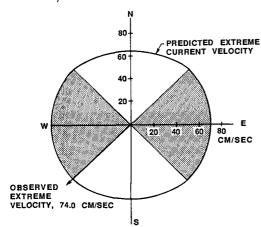


Figure 11: Computed extreme current velocities expected in a four-month observation for various directions.

# CONCLUSIONS

From the results of the stochastic analysis of offshore current data the following conclusions can be drawn:

- (1) Deviations from the mean value of the current velocity for the East-West and North-South components (including both tidal and residual velocity components) obey a non-Gaussian probability distribution with parameter  $\lambda_4$  which is associated with the kurtosis of the distribution.
- (2) The correlation coefficient evaluated for the East-West and the North-South current velocity time histories is extremely small; hence they are considered to be statistically independent.

- (3) When the East-West and North-South velocity components are decomposed into high-frequency (tidal) and low-frequency (residual) components, the tidal and residual components of the current velocity are found to be statistically independent. Both the tidal and residual currents may be assumed to be Gaussian random processes. In particular, the residual component appears to be a non-narrow-band Gaussian random process.
- (4) Histograms of maxima (peak values) of fluctuating currents in all four directions (East, West, North, and South) indicate that the maxima (including both tidal and residual components) can be marginally represented by the distribution of the maxima for a narrow-band non-Gaussian random process. It appears that the maxima obey the distribution applicable for a non-narrow-band non-Gaussian random process.
- (5) The area under the spectral density function agrees well with the variance obtained from the time histories for both the East- West and North-South velocity components.
- (6) The statistical properties of current velocity obtained from analysis of current data at deeper depths are nearly the same as those obtained from near-surface current data. However, the non-Gaussian random process characteristics stated in Item (1) are substantially less pronounced at deeper depths.
- (7) The square-root of the current energy, which is proportional to the current velocity decreases exponentially with an increase in water depth. The rate of decrease is much larger for the residual current velocity than that for the tidal current velocity.
- (8) An approximate method for estimating the magnitude of extreme current velocity is developed by applying order statistics to the probability distribution of a non-Gaussian random process. The results of computations made for a 4-month observation period show satisfactory agreement with observed data.

#### ACKNOWLEDGEMENTS

This research was sponsered by the Office of Naval Research, Ocean Technology Program, through contracts N00014-86-k-0537 to the University of Florida. The authors would like to express their appreciation to Dr. E.A. Silva for his valuable technical discussions received during the course of this project. The authors are grateful to Dr. Max Sheppard for his kind help in obtaining the current data used in this study. The authors also wish to express their appreciation to Ms. Laura Dickinson for typing the manuscript.

# APPENDIX: PROBABILITY DISTRIBUTION OF CURRENT VELOCITY FOR AN ARBITRARY DIRECTION

The standardized non-Gaussian probability density function with the parameter  $\lambda_4$  can be written as

$$f(z) = \frac{1}{\sqrt{2\pi}} \exp\{-\frac{z^2}{2}\} \left[ 1 + \frac{\lambda_4}{4!} H_4(z) \right]$$
 (A.1)

where  $H_4(z) = z^4 - 6z^2 + 3$ .

mean, variance  $\sigma^2$ , and parameter  $\lambda_4$  becomes

$$\Phi_z(t) = \exp\{-\frac{\sigma^2 t^2}{2}\} (1 + \frac{\lambda_4}{4!} \sigma^4 t^4) \tag{A.3}$$

Next, let us consider two statistically independent non-Gaussian random variables  $x_e$  and  $x_n$ , representing the East-West current velocity and the North-South current velocity, respectively. These are,

$$x_e$$
: non-Gaussian $(0, \sigma_e^2; \lambda_{4e})$   
 $x_n$ : non-Gaussian $(0, \sigma_n^2; \lambda_{4n})$  (A.4)

We may then write the current velocity for an arbitrary direction  $\theta$  as

$$x(\theta) = x_e \sin\theta + x_n \cos\theta \tag{A.5}$$

where  $\theta$  = angle measured from North to East.

Since  $x_e$  and  $x_n$  are statistically independent, the characteristic function of  $x(\theta)$  can be obtained by applying Eq.(A.3) as

$$\begin{split} \Phi_{x(\theta)}(t) &= \Phi_{xe}(t\sin\theta) \cdot \Phi_{xn}(t\cos\theta) \\ &\sim \exp\left\{-(\sigma_e^2 \sin^2\theta + \sigma_n^2 \cos^2\theta) \frac{t^2}{2}\right\} \\ &\qquad \qquad x \left[1 + \frac{1}{4!} (\lambda_{4e} \sigma_e^4 \sin^4\theta + \lambda_{4n} \sigma_n^4 \cos^4\theta) t^4\right] \\ &= \exp\left\{-(\sigma_e^2 \sin^2\theta + \sigma_n^2 \cos^2\theta) \frac{t^2}{2}\right\} \\ &\qquad \qquad x \left[1 + \frac{1}{4!} \frac{\lambda_{4e} \sigma_e^4 \sin^4\theta + \lambda_{4n} \sigma_n^4 \cos^4\theta}{(\sigma_e^2 \sin^2\theta + \sigma_n^2 \cos^2\theta)^2} \right] \\ &\qquad \qquad x \left[\tau_e^2 \sin^2\theta + \sigma_n^2 \cos^2\theta\right] \\ &\qquad \qquad x \left[\tau_e^2 \sin^2\theta + \sigma_n^2 \cos^2\theta\right] \end{split}$$

From a comparison of Eqs.(A.3) and (A.6), it can be proved that the random variable  $x(\theta)$  has approximately a non-Gaussian distribution with the following variance,  $\sigma^2(\theta)$ , and parameter,  $\lambda_4(\theta)$ :

$$\sigma^{2}(\theta) = \sigma_{e}^{2} \sin^{2} \theta + \sigma_{n}^{2} \cos^{2} \theta$$

$$\lambda_{4}(\theta) = \frac{\lambda_{4e} \sigma_{e}^{4} \sin^{4} \theta + \lambda_{4n} \sigma_{n}^{4} \cos^{4} \theta}{(\sigma_{e}^{2} \sin^{2} \theta + \sigma_{n}^{2} \cos^{2} \theta)^{2}}$$
(A.7)

#### REFERENCES

- Beardlsey, R.C., and B. Butman, "Circulation on the New England Continental Shelf: Response to Strong Winter Storms," Geophysical Research Letter, Vol. 1, 1974, pp. 181-184.
- 2. Smith, R.L., "A Description of Current, Wind, and Sea Level Variations During Coastal Upwelling Off the Oregon Coast, July-August 1972," Journal of Geophysical Research, Vol. 79, 1974, pp. 435-443.
- Lee, T.N. and D.A. Mayer, "Low-Frequency Current Variability and Spin-Off Eddies Along the Shelf Off Southeast Florida," Journal Marine Res., Vol. 35, 1977, pp. 193-218.
- Chuang, W-S., D-P. Wang and W.C. Boicourt, "Low-Frequenct Current Variablity on the Southern Mid-Atlantic Bight," Journal of Physical Oceanography, Vol. 9, 1979, pp. 1144-1154.
- Hayes, S.P., "Variablity of Current and Bottom Pressure Across the Continental Shelf in the Northeast Gulf of Alaska," Journal of Physical Oceanography, Vol. 9. 1979, pp.88-103.
- Mayer, D.A., D.V. Hansen and D. Ortman, "Long-Term Current and Temperature Observations on the Middle Atlantic Shelf," Journal of Geophysical Research, Vol. 84, 1979, pp.1776-1792.
- 7. Noble, M. and B. Butman, "On the Longshelf Structure and Dynamics of Subtidal Currents on the Eastern United States Continental Shelf," Journal of Physical Oceanography, Vol. 13, 1983, pp. 2125-2147.
- 8. Butman, B. and R.C. Beardsley, "Long-Term Observations on the Southern Flank of Georges Bank. Part 1: A Description of the Seasonal Cycle of Currents, Temperature, Stratification, and Wind Stress," Journal of Physical Oceanography, Vol. 17, 1987, pp. 367-384.
- Edgeworth, F.Y., "On the Representation of Statistical Frequency by a Series," Journal, Royal Statistical Society Series A, Vol 70, 1907, pp. 102-106.
- Longuet-Higgens, M.S., "The Effect of Non-Linearities on Statistical Distribution in the Theory of Sea Waves," Journal of Fluid Mechanics, Vol. 17. Part 3, 1963, pp.459-480.
- Ochi, Michel K. and W-C. Wang, "Prediction of Wave Height of Wind-Generated Seas in Infinite Water Depth," Tech. Rep. UFL/COEL/TR-052, University of Florida, 1984.